

The QED contribution to J/ψ plus light hadrons production at B-factories

Zhi-Guo He¹ and Jian-Xiong Wang²

¹ *II. Institut für Theoretische Physik, Universität Hamburg,*

Luruper Chaussee 149, 22761 Hamburg, Germany

²*Institute of High Energy Physics, Chinese Academy of Science,*

P.O. Box 918(4), Beijing, 100049, China.

Theoretical Physics Center for Science Facilities, (CAS) Beijing, 100049, China.

(Dated: January 21, 2013)

Abstract

To understand the direct $J/\psi + X_{\text{non-}c\bar{c}}$ production mechanism in e^+e^- annihilation, in this work, we propose to measure the inclusive J/ψ plus light hadrons (LH) production at B-factories and present a detailed study on its QED production due to $\psi(2S)$ feed-down, where the $\psi(2S)$ are produced in $e^+e^- \rightarrow \psi(2S) + \gamma$ and $e^+e^- \rightarrow \psi(2S) + f\bar{f}$, $f = \text{lepton, lightquark}$, and QED contribution to direct $J/\psi + q\bar{q}$ production with $q = u, d, s$ quark. We find that the QED contribution is huge in the whole phase space region, but can be reduced largely and is in the same order as the QCD contribution when a suitable cut on the angle $\theta_{J/\psi}$ between J/ψ and the e^+e^- beam is made. In this way, the cross section of $J/\psi + LH$ QCD production can be obtained by subtracting the QED contribution from the experimental measurement on inclusive J/ψ plus light hadrons. To help to remove the QED background, we also calculate the angular and momentum distribution of J/ψ in the QED contribution.

PACS numbers: 12.38.Bx, 13.66.Bc, 14.40.Pq

I. INTRODUCTION

The development of the non-relativistic QCD (NRQCD) effective field theory [1] provides a powerful tool to study the production and decay of heavy quarkonium states that are constituted by one heavy quark (Q) and one heavy anti-quark \bar{Q} . The virtual difference between NRQCD and the conventional color-singlet model (CSM) is that it allows the contribution of $Q\bar{Q}$ state in the color-octet (CO) configuration at short-distance which finally evolves into heavy mesons through emission of soft gluon(s) non-perturbatively. This is referred as the CO mechanism (COM). The role of the COM has been extensively studied in various high energy environments, for reviews see Ref.[2].

Among them, the J/ψ production in e^+e^- annihilation at B-factories (the Babar and Belle) have attracted considerable solicitude in recent years. Experimentally, the cross section for inclusive J/ψ production was reported by the Babar [3] and Belle [4] collaborations in 2001. Belle collaboration further divided the inclusive J/ψ production rate into two pieces: (a) $e^+e^- \rightarrow J/\psi + c\bar{c}$ part^a, (b) $e^+e^- \rightarrow J/\psi + X_{\text{non-}c\bar{c}}$ part, and measured them separately [5, 6]. The latest results reported by the Belle are [6]

$$\sigma(e^+e^- \rightarrow J/\psi + X) = 1.17 \pm 0.02 \pm 0.07\text{pb}, \quad (1a)$$

$$\sigma(e^+e^- \rightarrow J/\psi + c\bar{c} + X) = 0.74 \pm 0.08_{-0.08}^{+0.09}\text{pb}, \quad (1b)$$

$$\sigma(e^+e^- \rightarrow J/\psi + X_{\text{non-}c\bar{c}}) = 0.43 \pm 0.09 \pm 0.09\text{pb}. \quad (1c)$$

In the case of $J/\psi + c\bar{c}$ production, where the the CO contribution is found to be very small [9], there were large discrepancies between Belle results and NRQCD predictions at leading order (LO) in α_s and v [8–10], where v is the relative velocity between c and \bar{c} in the meson rest frame. These puzzles are now largely resolved after taking into account the next-to-leading order (NLO) QCD corrections [11, 12] and the relativistic corrections [13]. In contrast, in the $J/\psi + X_{\text{non-}c\bar{c}}$ production case, the contribution of the CO $e^+e^- \rightarrow c\bar{c}(^1S_0, ^3P_J^0) + g$ [14–17] process is expected to be significant and even larger than that of the CS $e^+e^- \rightarrow c\bar{c}(^3S_1^0) + gg$ process. At LO, the cross sections of the CO and CS processes are predicted to be about $0.3 \sim 0.8\text{pb}$ and $0.2 \sim 0.3\text{pb}$ [8, 18], respectively.

^a Here the $J/\psi + c\bar{c}$ includes both the exclusive double charmonium production process and the J/ψ production process in association with charmed hadrons, and the cross section for double charmonium production process was also reported by Babar collaboration later [7].

Recently, the k-factor of their NLO QCD corrections were found to be about 1.3 [19, 20] and 1.9 [21] correspondingly, and what's more the relativistic corrections can also enhance the LO CS result by about 20% – 30% [22, 23]. Then up to the NLO of α_s and v^2 , the cross section of the CS contribution itself can reach about $440 \sim 560\text{fb}$ [22]. which almost saturate the Belle measurement and leave very little room for CO contribution. So in $e^+e^- \rightarrow J/\psi + X_{\text{non-}c\bar{c}}$ process, there is a large conflict between NRQCD prediction and Belle current measurements. By setting the CS contribution into zero, the upper limit of the CO matrix elements is obtained [21]

$$\langle 0|\mathcal{O}(^1S_0^8)|0\rangle^{J/\psi} + 4.0\langle 0|\mathcal{O}(^3P_J^8)|0\rangle^{J/\psi}/m_c^2 < (2.0 \pm 0.6) \times 10^{-2}\text{GeV}^3. \quad (2)$$

However, in some other processes of J/ψ production, the recent theoretical calculations shown that the CO contribution is important. For example, (a) for J/ψ production from Z decay, the CS result at QCD NLO [24], can only account for one-half of the experimental data and the other half might be attributed to the CO contribution; (b) for J/ψ production in Υ decay, there is large gap between CS contribution [25] and the experimental result; (c) for J/ψ photoproduction at HERA, the transverse momentum (p_t) distribution and the polarization parameters of J/ψ can not be well described by the CS channel at QCD NLO alone as well [26, 27], and the NRQCD prediction that includes both the CO and CS contributions can give a well description of the J/ψ p_t distribution when the NLO QCD corrections are taken into account [28]; (d) for J/ψ hadroproduction, despite of the huge NLO QCD corrections [29–31], the CS contribution still can not explain the experimental measurements, and the role of the COM is significant [32–35]. By fitting the J/ψ hadroproduction data with the complete NRQCD results at QCD NLO, including both the CS and CO contributions, two different sets of constraint for the CO matrix elements are obtained, which are $\langle 0|\mathcal{O}(^1S_0^8)|0\rangle^{J/\psi} + 3.9\langle 0|\mathcal{O}(^3P_J^8)|0\rangle^{J/\psi}/m_c^2 = 7.4 \times 10^{-2}\text{GeV}^3$ [34], and $\langle 0|\mathcal{O}(^1S_0^8)|0\rangle^{J/\psi} + 3.9\langle 0|\mathcal{O}(^3P_J^8)|0\rangle^{J/\psi}/m_c^2 = 2.4 \times 10^{-2}\text{GeV}^3$ [35]. Although these two results are not consistent with each other, both of them exceed the upper limit given in Eq.(2). In particular, the former one is three times larger than the limit in Eq.(2). These studies yield almost completely opposite conclusion about how large the CO contribution is, or in other words, how large the values of the CO matrix elements could be.

After comparing the results of the Babar and Belle with the theoretical calculation meticulously, we find that there are some uncertainties which can potentially have large impact

on the current conclusion. One is that the Babar measurement on J/ψ inclusive production cross section [3] is about two times larger than that of Belle[6]. If we subtract the measurement of the Belle $\sigma(J/\psi + c\bar{c} + X) = 0.74\text{pb}$, which is well understood theoretically, from Babar result, there will be enough room left for CO contribution. One possible reason for the different results of the Babar and Belle is that they use different methods to select the data. Another uncertainty is that, in the latest measurement of the Belle [6], they only select the event that includes at least five charge tracks in the final states, and make no corrections. This means that all events that include zero or two charged light hadrons, such as $J/\psi + m(\pi^+\pi^-) + n\pi^0$ for $(m = 0, 1; n = 0, 1, 2 \dots)$, are excluded. From the point view of quark-hadron duality, Belles measurements do not include the whole NRQCD predictions. It may has little influence on the measurement of $\sigma(e^+e^- \rightarrow J/\psi + c\bar{c})$ [6], but large influence on that of $\sigma(e^+e^- \rightarrow J/\psi + X_{\text{non-}c\bar{c}})$ from the non-perturbative hadronization mechanism of gluons. To reduce the uncertainties mentioned above and understand the $J/\psi + X_{\text{non-}c\bar{c}}$ production mechanism, we suggest to measure the cross section of $J/\psi + \text{light hadrons (LH)}$ production by the Belle and Babar collaborations with the same kinematic criteria, which can be compared with the theoretical prediction directly.

Besides the interesting conventional QCD contribution, there are also large QED backgrounds due to $\psi(2S) \rightarrow J/\psi + \pi\pi^b$, where $\psi(2S)$ is produced in the initial state radiation (ISR) process $e^+e^- \rightarrow \psi(2S) + \gamma$ and higher order QED processes $e^+e^- \rightarrow \psi(2S) + f\bar{f}$ (f can be lepton or light quark), and direct J/ψ production in the $e^+e^- \rightarrow 2\gamma^* \rightarrow J/\psi + q\bar{q}$ process with $q = u, d, s$ quark. To help to remove them, in this work, we will present a detailed study about the $\psi(2S)$ and $J/\psi + q\bar{q}$ productions in the QED processes and their influence on the $J/\psi + \text{LH}$ measurement.

II. FRAMEWORK OF CALCULATION

For the process of $J/\psi + \pi\pi$ production from $\psi(2S)$ feed-down, the Feynman amplitude \mathcal{M} can be generally written as:

$$\mathcal{M} = \mathcal{M}_\mu^{\psi(2S)}(P_{2S}) \times \frac{-g^{\mu\nu} + \frac{P_{2S}^\mu P_{2S}^\nu}{P_{2S}^2}}{P_{2S}^2 - M_{2S}^2 + i * M_{2S}\Gamma} \mathcal{M}_\nu^{(\psi(2S) \rightarrow J/\psi + \pi\pi)} \quad (3)$$

^b $\psi(2S)$ can also decay into $J/\psi + \eta$. However the branching ratio is more 15 times smaller than the 2π channel, so we do not take it into account in our calculation.

where $\mathcal{M}_\mu^{\psi(2S)}$ (P_{2S}) and $\mathcal{M}_\nu^{\psi(2S)\rightarrow J/\psi+\pi\pi}$ are the Feynman amplitudes for $\psi(2S)$ production with momentum P_{2S} and $\psi(2S)$ decay into $J/\psi + \pi\pi$ respectively, and Γ is the total decay width of $\psi(2S)$. Using narrow width approximation

$$\lim_{\Gamma\rightarrow 0} \frac{1}{(P_{2S}^2 - M_{2S}^2)^2 + M_{2S}^2 \Gamma^2} = \frac{\pi\delta(P_{2S}^2 - M_{2S}^2)}{M_{2S}\Gamma}, \quad (4)$$

it is straightforward to obtain the expression for the corresponding cross section which is factorized as the product of the cross section of $\psi(2S)$ production and the branching function of $\psi(2S) \rightarrow J/\psi + \pi\pi$:

$$\sigma = \frac{1}{8s} \int \sum |\mathcal{M}^{\psi(2S)}|^2 d\text{LIPS}_1 \times \frac{1}{2(2J+1)M_{2S}\Gamma} \int \sum |\mathcal{M}^{\psi(2S)\rightarrow J/\psi+\pi\pi}|^2 d\text{LIPS}_2, \quad (5)$$

where LIPS_1 is the phase space of $\psi(2S)$ production, LIPS_2 is the phase space of $\psi(2S)$ decay into $J/\psi + \pi\pi$, and $J = 1$ is the spin of $\psi(2S)$.

We use the effective Lagrangian that is constructed in Ref.[39] to describe $\psi(2S) \rightarrow J/\psi + \pi\pi$. The amplitude $\mathcal{M}^{\psi(2S)\rightarrow J/\psi+\pi\pi}$ can be read directly from the Lagrangian

$$\begin{aligned} \mathcal{M}^{\psi(2S)\rightarrow J/\psi+\pi(p_1)\pi(p_2)} = & -\frac{4}{F_0^2} \left[\left(\frac{g}{2}(m_{\pi\pi}^2 - 2M_\pi^2) + g_1(v \cdot p_1)(v \cdot p_2) + g_3 M_\pi^2 \right) \right. \\ & \left. \times \epsilon_{J/\psi}^* \cdot \epsilon_{\psi(2S)} + g_2(p_{1\mu}p_{2\nu} + p_{1\nu}p_{2\mu})\epsilon_{J/\psi}^{*\mu}\epsilon_{\psi(2S)}^\nu \right] \end{aligned} \quad (6)$$

where $m_{\pi\pi}^2 = (p_1 + p_2)^2$, M_π is the mass of π meson, and $v = (1, \vec{0})$ in the rest frame of $\psi(2S)$. In their convention, the π decay constant $F_0 \simeq 93\text{MeV}$. The coupling constant $g_2 \simeq 0$, because it is strongly suppressed by the chiral symmetry breaking scale over m_c . By fitting the distributions of $m_{\pi\pi}$ and $\cos\theta_\pi^*$, which is the angle between J/ψ and π^+ in the rest frame of $\psi(2S)$, in the decay of $\psi(2S) \rightarrow J/\psi + \pi^+\pi^-$, the BES Collaboration obtained two set results for $\frac{g_1}{g}$ and $\frac{g_3}{g}$ [40]. Together with $\text{Br}(\psi(2S) \rightarrow J/\psi + \pi^+\pi^-) = 33.6\%$ [41], they then obtained that^c

$$g = 0.322, \quad \frac{g_1}{g} = -0.49, \quad \frac{g_3}{g} = 0.54, \quad (7)$$

or

$$g = 0.319, \quad \frac{g_1}{g} = -0.347, \quad g_3 = 0. \quad (8)$$

For the processes considered, $\mathcal{M}^{\psi(2S)\rightarrow J/\psi+\pi\pi}$ is common, so we essentially only need to compute \mathcal{M}^{2S} . In the non-relativistic limit, for the QED process of $e^+e^- \rightarrow \psi(2S) + X$ the

^c These parameters can also well reproduce the decay width of $\psi(2S) \rightarrow J/\psi + \pi^0\pi^0$.

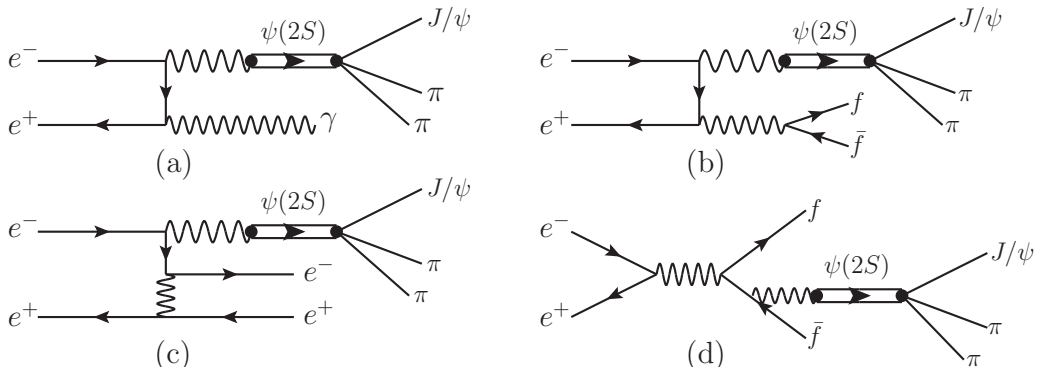


FIG. 1: The typical diagrams describing the $\psi(2S)$ feed-down background.

factorization formula in CSM and NRQCD are equivalent, and the amplitude $\mathcal{M}^{\psi(2S)}$ can be written as:

$$\mathcal{M}^{\psi(2S)} = \sqrt{C_{2S}} \sum_{s_1, s_2} \sum_{i, j} \langle s_1; s_2 | 1 S_z \rangle \langle 3i; \bar{3}j | 1 \rangle \mathcal{M}(e^+e^- \rightarrow c_i(\frac{P_{2S}}{2}, s_1) + \bar{c}_j(\frac{P_{2S}}{2}, s_2) + X) \quad (9)$$

where \mathcal{M} is the standard Feynman amplitude for $e^+e^- \rightarrow c_i(\frac{P_{2S}}{2}, s_1) + \bar{c}_j(\frac{P_{2S}}{2}, s_2) + X$, $\langle 3i; \bar{3}j | 1 \rangle = 1/\sqrt{N_c}$ and $\langle s_1; s_2 | 1 S_z \rangle$ are the SU(3)-color and SU(2)-spin Clebsch-Gordan coefficients for $c\bar{c}$ projecting on the CS spin-triplet S-wave state. The projection of Dirac spinors can be re-expressed as:

$$\sum_{s_1, s_2} \langle s_1; s_2 | 1 S_z \rangle v(\frac{P_{2S}}{2}, s_2) \bar{u}(\frac{P_{2S}}{2}, s_1) = \frac{1}{2\sqrt{2}} \not{\epsilon}^*(S_z) (P_{2S} + M_{2S}). \quad (10)$$

C_{2S} can be related to the $\psi(2S)$ wave function at origin by $C_{2S} = \frac{1}{4\pi} |R_{2S}(0)|$. And $|R_{2S}(0)|$ can be obtained from potential model calculation or can be determined from $\psi(2S)$ decay into e^+e^- with

$$\Gamma(\psi(2S) \rightarrow e^+e^-) = \frac{16\alpha^2 |R_{2S}(0)|^2}{9M_{2S}^2} \quad (11)$$

III. THE FEED-DOWN BACKGROUND FROM $e^+e^- \rightarrow \psi(2S) + \gamma$

The typical Feynman diagrams for the ISR process $e^+e^- \rightarrow \psi(2S) + \gamma$ followed by $\psi(2S) \rightarrow J/\psi + \pi\pi$ are shown in Fig.(1a). Using the formula introduced in Eq.(5-8), we

compute $|\mathcal{M}(e^+e^- \rightarrow \psi(2S) + \gamma)|^2$ analytically and obtain

$$|\mathcal{M}(e^+e^- \rightarrow \psi(2S) + \gamma)|^2 = \frac{96e_c^2(4\pi\alpha)^3 C_{2S}}{s r (-1+r+(-1+r)(-1+4r_e)x_2^2)^2} \left(-1-2r-r^2 -8r_e+16rr_e+32r_e^2-4(r+2r_e)(-1+4r_e)x_2^2+(-1+r)^2(1-4r_e)^2x_2^4 \right) \quad (12)$$

where $e_c = \frac{2}{3}$, $r = \frac{M_{2S}^2}{s}$, $r_e = \frac{m_e^2}{s}$, $x_2 = \cos(\theta_{\psi(2S)})$ and $\theta_{\psi(2S)}$ is the angel between $\psi(2S)$ and the e^+e^- beam. In the limit of $r_e = 0$, Eq.(12) can be simplified as:

$$|\mathcal{M}(e^+e^- \rightarrow \psi(2S) + \gamma)|^2 = \frac{96e_c^2(4\pi\alpha)^3 C_{2S}}{s} \left(\frac{1}{r} - \frac{2(1+r^2)}{r(1-r)^2(1-x_2^2)} \right). \quad (13)$$

Setting $M_{2S} = 3.686\text{GeV}$, $m_e = 0.51\text{MeV}$, $\alpha = \frac{1}{137}$, and using $\Gamma(\psi(2S) \rightarrow e^+e^-) = 4.30\text{keV}$, we get

$$\sigma(e^+e^- \rightarrow \psi(2S) + \gamma) = 13.22\text{pb}. \quad (14)$$

And the feed-down production

$$\sigma(e^+e^- \rightarrow \psi(2S) + \gamma) \times Br(\psi(2S) \rightarrow J/\psi + \pi\pi) = 6.79\text{pb}, \quad (15)$$

which, as expected, is huge. This is because in the limit of $m_e \rightarrow 0$, there will be collinear singularities in $|\mathcal{M}(e^+e^- \rightarrow \psi(2S) + \gamma)|^2$ in Eq.(13) at $x_2 = \pm 1$ points. The angular distribution $\frac{d\sigma(e^+e^- \rightarrow \psi(2S) + \gamma)}{dx_2}$ is shown in Fig.[2]. It can be found from Fig.[2] that the differential cross section drops down very fast when $\psi(2S)$ goes off the beam line a little. If we make a cut on x_2 , i.e the angle $\theta_{\psi(2S)}$, the cross section will be reduced largely. The cross sections in different cut conditions are given below:

$$\sigma(e^+e^- \rightarrow \psi(2S) + \gamma) \times Br(\psi(2S) \rightarrow J/\psi + \pi\pi) \Big|_{\frac{\pi}{18} < \theta_{\psi(2S)} < \frac{17\pi}{18}} = 1.48\text{pb}, \quad (16a)$$

$$\sigma(e^+e^- \rightarrow \psi(2S) + \gamma) \times Br(\psi(2S) \rightarrow J/\psi + \pi\pi) \Big|_{\frac{\pi}{9} < \theta_{\psi(2S)} < \frac{8\pi}{9}} = 0.99\text{pb}, \quad (16b)$$

$$\sigma(e^+e^- \rightarrow \psi(2S) + \gamma) \times Br(\psi(2S) \rightarrow J/\psi + \pi\pi) \Big|_{\frac{\pi}{6} < \theta_{\psi(2S)} < \frac{5\pi}{6}} = 0.71\text{pb}. \quad (16c)$$

Let $p_{J/\psi}^{*\mu}$ denotes the four-momentum of J/ψ in the rest frame of $\psi(2S)$, then $|\vec{\mathbf{p}}_{J/\psi}^*|/E_{J/\psi}^*$, the three-velocity of J/ψ , ranges from 0 to 0.15, which is much smaller than that of $\psi(2S)$ in the center of mass frame (CMF) of e^+e^- collision, which is about 0.78. So the angular distribution of J/ψ can be obtained approximately by setting $\theta_{\psi(2S)} = \theta_{J/\psi}$, where $\theta_{J/\psi}$ is the angel between J/ψ and the e^+e^- beam. However, such an approximation may not be good enough here, because the cross section of $J/\psi + \pi\pi$ produced from the feed-down of $\psi(2S)$

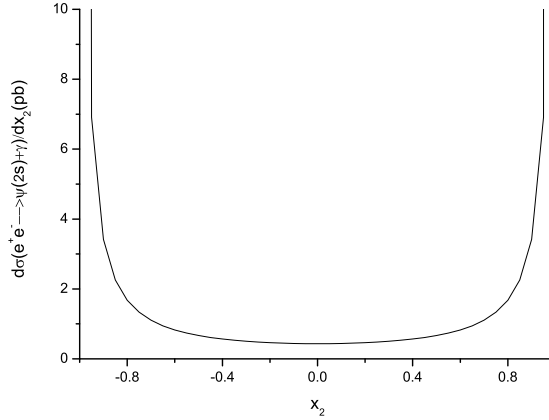


FIG. 2: The angular distribution of $\psi(2S)$ in the ISR process $e^+e^- \rightarrow \psi(2S) + \gamma$, where $x_2 = \cos(\theta_{\psi(2S)})$, and $\theta_{\psi(2S)}$ is the angular between $\psi(2S)$ and the e^+e^- beam.

ISR process (Eq.(15)) is more than 10 times larger than that of the CS QCD process[22], and a tiny difference may potentially result in a considerable effect. In this work, we calculated it directly. In the CMF, $x'_2 = \cos(\theta_{J/\psi})$, can be expressed as:

$$x'_2 = \frac{\mathbf{k}_1 \cdot \mathbf{p}'_{J/\psi}}{|\mathbf{k}_1| |\mathbf{p}'_{J/\psi}|}, \quad p'_{J/\psi} = L p_{J/\psi}^* \quad (17)$$

where k_1 is the four-momentum of e^+ , L is the Lorentz transformation from $\psi(2s)$ rest frame to the CMF. $p'_{J/\psi}$ is the J/ψ four-momentum in the CMF. To do the calculation, the formula for the decay $\psi(2s) \rightarrow J/\psi + \pi\pi$ and $\psi(2s)$ production are placed in the numerical phase space integration program generated by using the Feynman Diagram Calculation (FDC) package [42], in which the Lorentz transformation and the cut conditions are employed in the numerical calculation. The decay $\psi(2s) \rightarrow J/\psi + \pi\pi$ is calculated by using Eq.(6) with $M_{\pi^+} = M_{\pi^-} = 140\text{MeV}$ and $M_{\pi^0} = 135\text{MeV}$. When parameter set in Eq.(7) are used, the cross sections in different cut conditions are

$$\sigma(e^+e^- \rightarrow (J/\psi + \pi\pi)_{\psi(2S)} + \gamma) \Big|_{\frac{\pi}{18} < \theta_{J/\psi} < \frac{17\pi}{18}} = 1.51\text{pb}; \quad (18a)$$

$$\sigma(e^+e^- \rightarrow (J/\psi + \pi\pi)_{\psi(2S)} + \gamma) \Big|_{\frac{\pi}{9} < \theta_{J/\psi} < \frac{8\pi}{9}} = 0.99\text{pb}; \quad (18b)$$

$$\sigma(e^+e^- \rightarrow (J/\psi + \pi\pi)_{\psi(2S)} + \gamma) \Big|_{\frac{\pi}{6} < \theta_{J/\psi} < \frac{5\pi}{6}} = 0.71\text{pb}. \quad (18c)$$

Alternatively, if we choose the parameter set in Eq.(8), the corresponding cross sections become:

$$\sigma(e^+e^- \rightarrow (J/\psi + \pi\pi)_{\psi(2S)} + \gamma) \Big|_{\frac{\pi}{18} < \theta_{J/\psi} < \frac{17\pi}{18}} = 1.52\text{pb}; \quad (19a)$$

$$\sigma(e^+e^- \rightarrow (J/\psi + \pi\pi)_{\psi(2S)} + \gamma) \Big|_{\frac{\pi}{9} < \theta_{J/\psi} < \frac{8\pi}{9}} = 1.00\text{pb}; \quad (19b)$$

$$\sigma(e^+e^- \rightarrow (J/\psi + \pi\pi)_{\psi(2S)} + \gamma) \Big|_{\frac{\pi}{6} < \theta_{J/\psi} < \frac{5\pi}{6}} = 0.71\text{pb}. \quad (19c)$$

The numerical results in Eq.(16,18,19) show that for $J/\psi + \pi\pi$ production from the ISR $\psi(2S)$ feed-down process the approximation

$$\frac{d\sigma(e^+e^- \rightarrow (J/\psi + \pi\pi)_{\psi(2S)} + \gamma)}{d \cos(\theta_{J/\psi})} = \frac{d\sigma(e^+e^- \rightarrow \psi(2S) + \gamma) \times Br(\psi(2S) \rightarrow J/\psi + \pi\pi)}{d \cos(\theta_{\psi(2S)})} \quad (20)$$

holds very well in the range of $\pi/9 < \theta_{J/\psi} < 8\pi/9$ at $\sqrt{s} = 10.6$ GeV, and the J/ψ angular distribution is almost not dependent on the details about how $\psi(2S)$ decays into $J/\psi + \pi\pi$. Hence the angular distribution of J/ψ can be safely obtained by using the angular distribution of $\psi(2S)$ in the interval $\pi/9 < \theta_{J/\psi} < 8\pi/9$ with an additional renormalization factor of branching ratio of $\psi(2S) \rightarrow J/\psi + \pi\pi$.

Because the energy difference between $\psi(2S)$ and J/ψ is at the same order as the energy of the soft gluon emitted from the CO $c\bar{c}({}^3P_J^8, {}^1S_0^8)$ states [1], which is of $m_c v^2$ order, there is a large overlap between the kinematic region of the J/ψ coming from ISR $\psi(2S)$ feed-down and that of the J/ψ produced in the CO process. To measure the CO J/ψ production, it is helpful to know the momentum distribution of J/ψ production in the feed-down from the ISR $\psi(2S)$ process. We calculate it numerically with different cut conditions of $\theta_{J/\psi}$ by using the two set of parameters in Eq.(7,8), and the results are given in Fig.[3(a)-3(d)]. The results in Fig.[3(a)-3(d)] show that similar to the angular distribution, the momentum spectra give almost same results for those two different parameter sets. Hence for simplicity, we only choose the parameter set in Eq.(7) in the following calculations.

IV. BACKGROUND FROM HIGHER QED PROCESSES

In direct J/ψ production, the background coming from higher QED processes $e^+e^- \rightarrow J/\psi + f + \bar{f}$ is also considerable [38], where f can be lepton or light quark, and therefore the feed-down background from $e^+e^- \rightarrow \psi(2S) + f + \bar{f}$ can not be ignored too. The typical

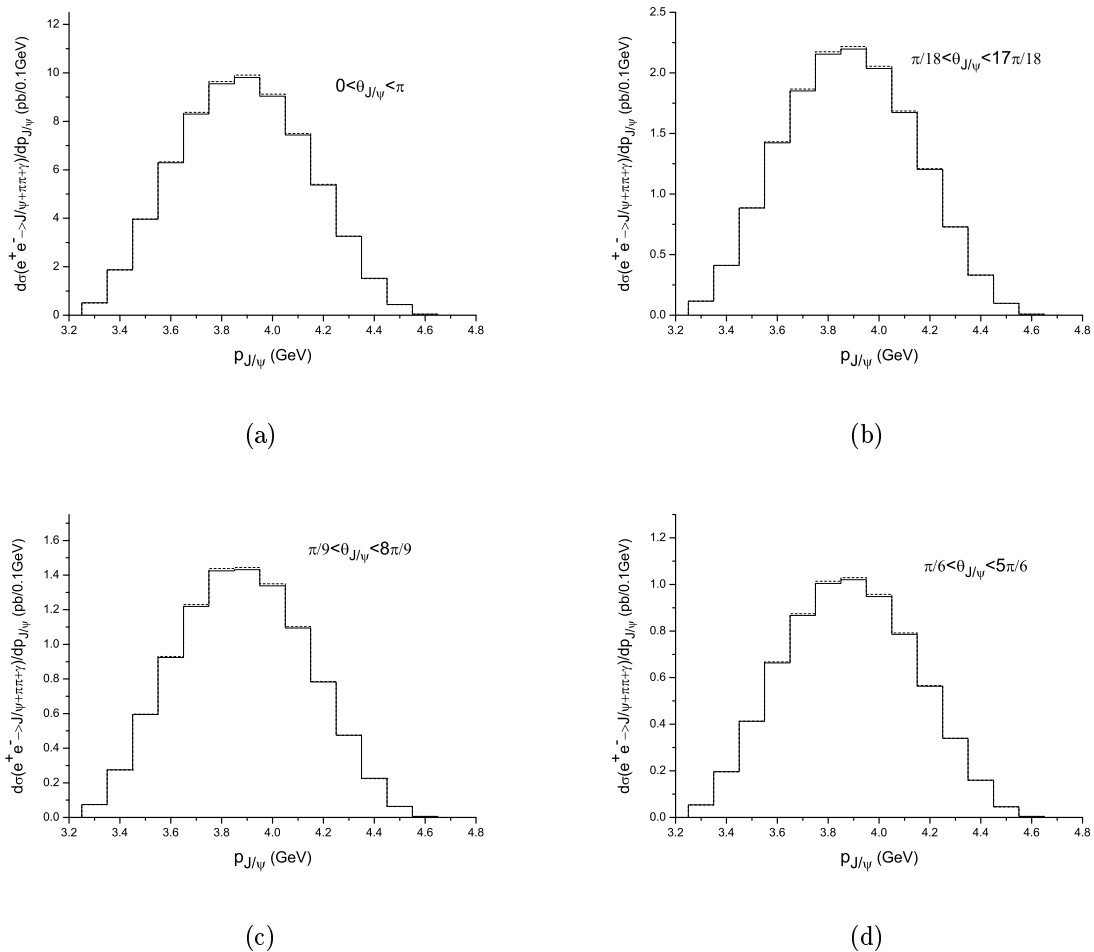


FIG. 3: The momentum spectra of J/ψ produced from the feed-down of ISR $\psi(2S)$ process in different cut condition of $\theta_{J/\psi}$ by using two different sets of parameters in Eq.(7) (solid line) and Eq.(8) (dashed line) to describe $\psi(2S) \rightarrow J/\psi + \pi\pi$.

Feynman diagrams for $f \neq e$ are shown in Fig.(1b) and Fig.(1d). When $f = e$, there are additional t-channel diagrams, the typical one of which is shown in Fig.(1c). Because of this t-channel enhancement, the cross section for $f = e$ is expected to be much larger than $f \neq e$ case. We will discuss $f = e$ and $f \neq e$ cases separately in the subsections. At this order, in addition to the $\psi(2S)$ feed-down, there is also sizable QED contribution from direct $J/\psi + q\bar{q}$ production with $q = u, d, s$ quark, about which we will discuss in subsection C.

A. The Feed-Down Background From $e^+e^- \rightarrow \psi(2S) + e^+e^-$

According to the interaction type of the initial e^+e^- , we divide the $e^+e^- \rightarrow \psi(2S) + e^+e^-$ process into three part: the t-channel part (Fig.(1c)), the two-photon channel part (Fig.(1b)), and the s-channel part (Fig.(1d)). It is easy to check that the Feynman amplitude for each part itself is gauge invariant. Compared to cross section σ^T for the t-channel part, the cross sections for the two-photon part σ^{TP} and the s-channel part σ^S are suppressed by the factors $\frac{M_{\psi(2S)}^2}{s}$, and $\frac{M_{\psi(2S)}^2}{s} \ln^{-2}(\frac{s}{4M_e^2})$ respectively, which are about 10^{-1} and 10^{-4} orders accordingly at $\sqrt{s} = 10.6\text{GeV}$. Choosing the same values for the parameters as in the ISR process, we obtained

$$\sigma^T(e^+e^- \rightarrow (J/\psi + \pi\pi)_{\psi(2S)} + e^+e^-) = 0.50 \text{ pb}; \quad (21a)$$

$$\sigma^{\text{TP}}(e^+e^- \rightarrow (J/\psi + \pi\pi)_{\psi(2S)} + e^+e^-) = 4.8 \times 10^{-2} \text{ pb}; \quad (21b)$$

$$\sigma^S(e^+e^- \rightarrow (J/\psi + \pi\pi)_{\psi(2S)} + e^+e^-) = 8.5 \times 10^{-4} \text{ pb}. \quad (21c)$$

which are consistent with the qualitative estimation. The contribution of the s-channel part is only ~ 1 fb order, which is about three times order less that the t-channel contribution, so we drop it in the later analysis.

If we make the same cut on the $\theta_{J/\psi}$, σ^T and σ^{TP} both drop down largely too:

$$\sigma^{\text{T(TP)}}(e^+e^- \rightarrow (J/\psi + \pi\pi)_{\psi(2S)} + e^+e^-) \Big|_{\frac{\pi}{18} < \theta_{J/\psi} < \frac{17\pi}{18}} = 0.11(0.019)\text{pb}; \quad (22a)$$

$$\sigma^{\text{T(TP)}}(e^+e^- \rightarrow (J/\psi + \pi\pi)_{\psi(2S)} + e^+e^-) \Big|_{\frac{\pi}{9} < \theta_{J/\psi} < \frac{8\pi}{9}} = 0.059(0.013)\text{pb}; \quad (22b)$$

$$\sigma^{\text{T(TP)}}(e^+e^- \rightarrow (J/\psi + \pi\pi)_{\psi(2S)} + e^+e^-) \Big|_{\frac{\pi}{6} < \theta_{J/\psi} < \frac{5\pi}{6}} = 0.039(0.010)\text{pb}. \quad (22c)$$

The angular distribution of $\psi(2S)$ in the t- and two-photon channel parts are shown in Fig.[4]. We find that in $\pi/9 < \theta_{J/\psi} < 8\pi/9$ region the angular distribution of the J/ψ production from feed-down can be obtained by using that of $\psi(2S)$ as well with an additional renormalization factor of $Br(\psi(2S) \rightarrow J/\psi + \pi\pi)$. Unlike the ISR process, $p_{J/\psi}$ ranges from 0 to 4.7 GeV, and the momentum spectra of J/ψ for the the t- and two-photon channel parts are shown in Fig.[5].

We also calculate the interference between the t-channel part and the two-photon part and find it is very small. The cross section of the interference part for $(J/\psi + \pi\pi)_{\psi(2S)} + e^+e^-$

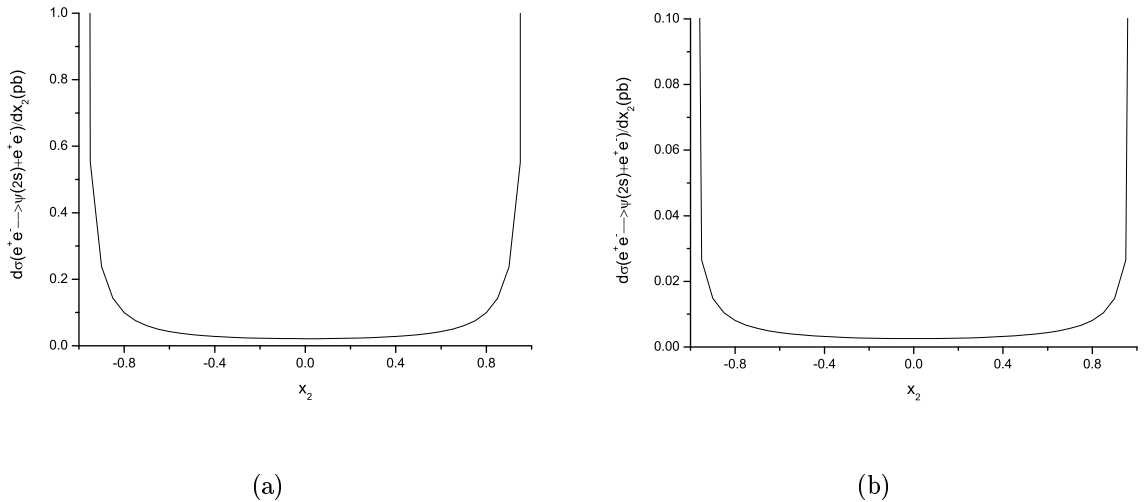


FIG. 4: The angular distribution of $\psi(2S)$ produced through t-channel (a), and two-photon channel (b) in the $e^+e^- \rightarrow \psi(2S) + e^+e^-$ process, where $x_2 = \cos(\theta_{\psi(2S)})$, and $\theta_{\psi(2S)}$ is the angular between $\psi(2S)$ and the e^+e^- beam.

is about -20fb in the whole phase space region. After including the interference part, the total cross section in different cut conditions of $\theta(J/\psi)$ are

$$\sigma(e^+e^- \rightarrow (J/\psi + \pi\pi)_{\psi(2S)} + e^+e^-) \Big|_{\frac{\pi}{18} < \theta_{J/\psi} < \frac{17\pi}{18}} = 0.12\text{pb}; \quad (23a)$$

$$\sigma(e^+e^- \rightarrow (J/\psi + \pi\pi)_{\psi(2S)} + e^+e^-) \Big|_{\frac{\pi}{9} < \theta_{J/\psi} < \frac{8\pi}{9}} = 0.070\text{pb}; \quad (23b)$$

$$\sigma(e^+e^- \rightarrow (J/\psi + \pi\pi)_{\psi(2S)} + e^+e^-) \Big|_{\frac{\pi}{6} < \theta_{J/\psi} < \frac{5\pi}{6}} = 0.047\text{pb}. \quad (23c)$$

The angular distribution of $\psi(2S)$ and momentum distribution of J/ψ for the whole process can be approximately obtained by adding the t- and two-photon channel contribution together respectively, because the interference effect is very small.

B. The Feed-Down Background From $e^+e^- \rightarrow \psi(2S) + f\bar{f}$ ($f \neq e$)

The process $e^+e^- \rightarrow \psi(2S) + f\bar{f}$ ($f \neq e$) has been fully studied in Ref.[43]. We also compute it independently and obtain consistent results:

$$\sum_{f=\mu,\tau,u,d,s} \sigma(e^+e^- \rightarrow (J/\psi + \pi\pi)_{\psi(2S)} + f\bar{f}) = 0.026\text{pb}. \quad (24)$$

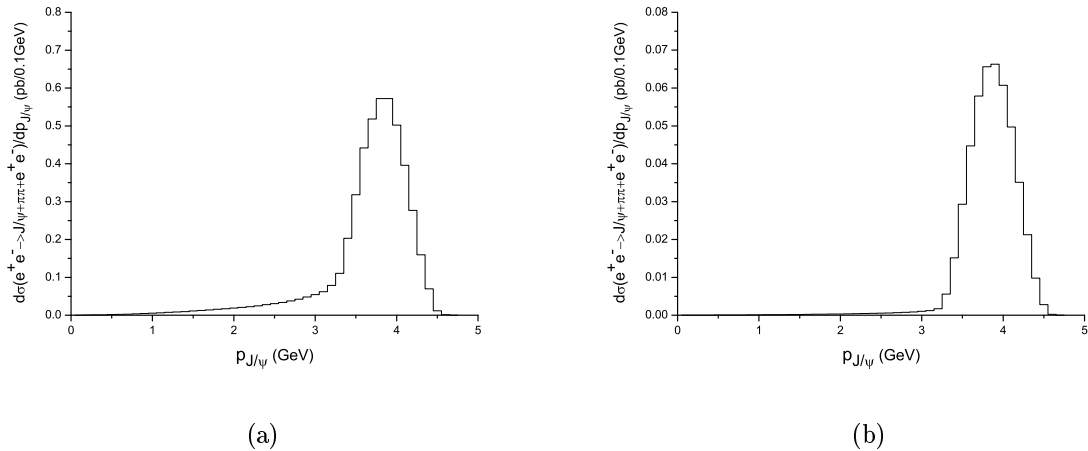


FIG. 5: The momentum distribution of J/ψ produced through the t-channel (a) and two-photon channel(b) in the $e^+e^- \rightarrow \psi(2S) + e^+e^-$ process.

If we make the same cut on the $\theta_{J/\psi}$, the cross section becomes:

$$\sum_{f=\mu,\tau,u,d,s} \sigma(e^+e^- \rightarrow (J/\psi + \pi\pi)_{\psi(2S)} + f\bar{f}) \Big|_{\frac{\pi}{18} < \theta_{J/\psi} < \frac{17\pi}{18}} = 0.020\text{pb}; \quad (25a)$$

$$\sum_{f=\mu,\tau,u,d,s} \sigma(e^+e^- \rightarrow (J/\psi + \pi\pi)_{\psi(2S)} + f\bar{f}) \Big|_{\frac{\pi}{9} < \theta_{J/\psi} < \frac{8\pi}{9}} = 0.015\text{pb}; \quad (25b)$$

$$\sum_{f=\mu,\tau,u,d,s} \sigma(e^+e^- \rightarrow (J/\psi + \pi\pi)_{\psi(2S)} + f\bar{f}) \Big|_{\frac{\pi}{6} < \theta_{J/\psi} < \frac{5\pi}{6}} = 0.011\text{pb}. \quad (25c)$$

The cross sections in different cut regions are within only about 0.020pb, which are about $4 \simeq 6$ times less than those in the $e^+e^- \rightarrow \psi(2S) + e^+e^-$ process, so small that we will not present further analysis here, and recommend Ref.[43] for more detailed results.

C. The Background From $e^+e^- \rightarrow J/\psi + q\bar{q}$

The Feynman diagrams for the $e^+e^- \rightarrow J/\psi + q\bar{q}$ process are similar to those for $e^+e^- \rightarrow \psi(2S) + q\bar{q}$ process. Since in the $\psi(2S)$ production process the contribution of the s-channel diagrams can be ignored, for the same reason, we will not consider it here too. The cross section of the $e^+e^- \rightarrow J/\psi + q\bar{q}$ has been calculated in Ref.[43], which is also considerable. Using the method introduced in Ref[43], we calculate the cross section with different cut

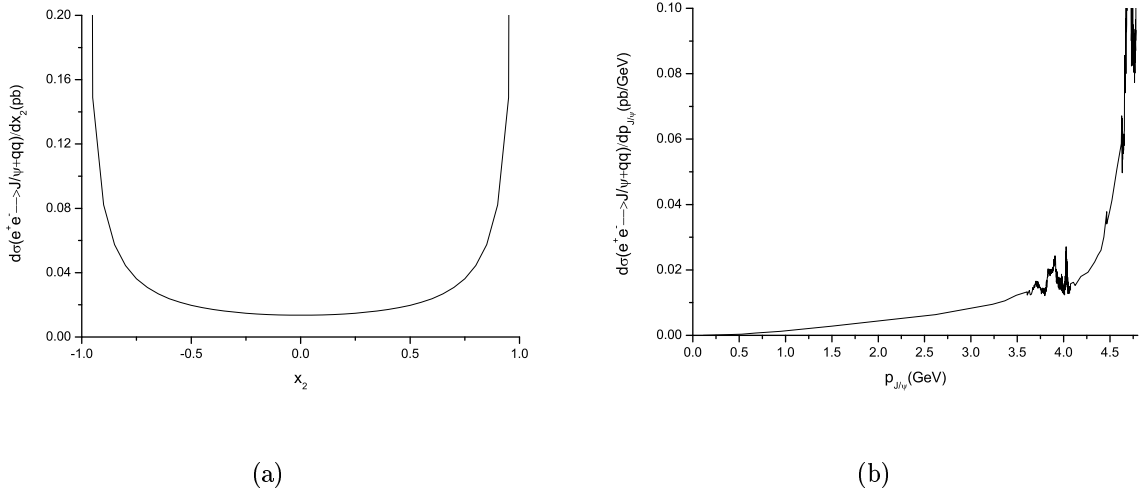


FIG. 6: The angular (a) and momentum (b) distributions of J/ψ in the process of $e^+e^- \rightarrow J/\psi + q\bar{q}$, where $x'_2 = \cos(\theta_{J/\psi})$, and $\theta_{J/\psi}$ is the angular between $\theta_{J/\psi}$ and the e^+e^- beam.

conditions of $\theta_{J/\psi}$:

$$\sum_{q=u,d,s} \sigma(e^+e^- \rightarrow J/\psi + q\bar{q}) \Big|_{\frac{\pi}{18} < \theta_{J/\psi} < \frac{17\pi}{18}} = 0.071 \text{pb}; \quad (26a)$$

$$\sum_{q=u,d,s} \sigma(e^+e^- \rightarrow J/\psi + q\bar{q}) \Big|_{\frac{\pi}{9} < \theta_{J/\psi} < \frac{8\pi}{9}} = 0.052 \text{pb}; \quad (26b)$$

$$\sum_{q=u,d,s} \sigma(e^+e^- \rightarrow J/\psi + q\bar{q}) \Big|_{\frac{\pi}{6} < \theta_{J/\psi} < \frac{5\pi}{6}} = 0.039 \text{pb}. \quad (26c)$$

The J/ψ angular and momentum distribution are shown in Fig.[6]. Note the difference between our results and those in Ref.[43] is due to the different choice of the parameters and the amount of data samples used in the R -value curve [41].

V. DISCUSSIONS AND CONCLUSIONS

Summing up the feed-down contribution from the ISR and $f\bar{f}$ processes and the contribution of direct $J/\psi + q\bar{q}$ production, the total QED background cross section are about

$$\sigma_{QED}(e^+e^- \rightarrow J/\psi + LH) = 7.46 \text{pb}, \quad (27)$$

which is more than one order of magnitude larger than the cross section of the conventional QCD production $e^+e^- \rightarrow J/\psi + LH$ [8, 19–21]. Such huge background make it difficult to

measure the QCD contribution in the whole phase space region. However, the background in the off beam region will drop down deeply. The cross section of the QED background in different cut regions are:

$$\sigma_{QED}(e^+e^- \rightarrow J/\psi + LH) \Big|_{\frac{\pi}{18} < \theta_{J/\psi} < \frac{17\pi}{18}} = 1.73\text{pb}; \quad (28a)$$

$$\sigma_{QED}(e^+e^- \rightarrow J/\psi + LH) \Big|_{\frac{\pi}{9} < \theta_{J/\psi} < \frac{8\pi}{9}} = 1.14\text{pb}; \quad (28b)$$

$$\sigma_{QED}(e^+e^- \rightarrow J/\psi + LH) \Big|_{\frac{\pi}{6} < \theta_{J/\psi} < \frac{5\pi}{6}} = 0.81\text{pb}. \quad (28c)$$

In NRQCD, the conventional $J/\psi + LH$ production includes the both the CS and the CO contribution. For the CS process $e^+e^- \rightarrow J/\psi + gg$, both the NLO QCD corrections[19] and relativistic corrections[22, 23] have been calculated. The cross section is found to be $0.4 \sim 0.7$ pb at NLO in α_s and v_c^2 [19, 20, 22]. The NLO QCD corrections to the CO contribution have also been obtained [21]. If we choose $\langle 0|\mathcal{O}(^1S_0^8)|0\rangle^{J/\psi} = (3.04 \pm 0.35) \times 10^{-2}\text{GeV}^3$, $\langle 0|\mathcal{O}(^3P_J^8)|0\rangle^{J/\psi} = (-9.08 \pm 1.61) \times 10^{-3}\text{GeV}^5$, which are obtained by a global fitting of J/ψ production data[44], the cross section of the CO contribution at α_s NLO will be about 0.3pb at $\mu = 2m_c, \alpha_s(\mu) = 0.245$. Then the total NRQCD prediction for the conventional $J/\psi + LH$ production will be about $0.7 \sim 1.0\text{pb}$. Unlike the QED background, the cut on $\theta_{J/\psi}$, for example $\pi/9 < \theta_{J/\psi} < 8\pi/9$, will only have a minor influence on the conventional QCD cross section σ^{QCD} , because both the CS and CO contribution do not depend strongly on $\theta_{J/\psi}$ [14, 20]. Therefore, we conclude that in a suitable cut condition of $\theta_{J/\psi}$, the cross section of the conventional QCD process can be in the same order as the background cross section. Furthermore, the results in [21] shown that CO contribution mainly assemble in the kinematic end point region, while the CS contribution is distributed in the whole region of $0 < p_{J/\psi} < 4.85\text{GeV}$, so to study the CO contribution, it can be further required $p_{J/\psi} > 3\text{GeV}$ in the measurement. Such a requirement will reduced the CS contribution by about 50%, but has little affect on the CO and the QED background contribution. In our calculation, we determine the effective vertices of $\psi(2S)\gamma^*$, $J/\psi\gamma^*$ and $\psi(2S) \rightarrow J/\psi + \pi\pi$ by fitting the experimental data and using the R -value to represent the effective vertex of $\gamma^*q\bar{q}$ in the calculation of $e^+e^- \rightarrow J/\psi(\psi(2S)) + q\bar{q}$ cross section, this indicates that all the possible important higher QCD correction effects to the background are included automatically, which makes the uncertainties of our result very small. Based on the above analysis, we think further measurement of the $J/\psi + LH$ production with a

suitable cut condition of $\theta_{J/\psi}$ and $p_{J/\psi}$ will be helpful to understand the role of the CO contribution to the J/ψ production mechanism in e^+e^- annihilation.

Recently the complete NLO QCD correction to the polarization of J/ψ hadroproduction were obtained by two groups [45, 46]. Due to their different ways of fitting the CO matrix elements, they got completely different conclusions. After taking into account the feed-down contribution of χ_{cJ} and $\psi(2S)$ states [47], the authors found that there is no solution to fit the p_t distribution of the cross section and J/ψ polarization measured by CDF collaboration simultaneously. Understanding the J/ψ production at B-factories can also help to resolve the polarization problem of J/ψ hadroproduction.

In summary, we study the dominant background sources of $J/\psi + \text{LH}$ production in e^+e^- annihilation, which include the ISR process $e^+e^- \rightarrow \psi(2S) + \gamma$ and higher QED process $e^+e^- \rightarrow \psi(2S) + f\bar{f}$, where f can be lepton or light quark, as well as the direct $e^+e^- \rightarrow J/\psi + q\bar{q}$ process with $q = u, d, s$ quark. We find that the cross section of the background process is very large in the whole phase space region. If we make a cut on the angle between J/ψ and e^+e^- beam, the cross section of the QED processes will reduced largely and become comparable to the cross section of the conventional QCD process. This indicates it is possible to measure the cross section of $J/\psi + \text{LH}$ from conventional QCD production at B-factories.

Acknowledgments

We would like to thank ChangZheng Yuan and Chao-Hsi Chang for helpful discussion. Z.G.He thanks the Theoretical Physics Center for Science Facilities(CAS) and Universitat de Barcelona for hospitality while part of this work was carried out. This work is supported by the National Natural Science Foundation of China (No. 10979056 and No.10935012), and by the Chinese Academy of Science under Project No. INFO-115-B01. The work of Z.G.He was supported in part by the CSD2007-00042 Consolider-Ingenio 2010 program under the CPAN08-PD14 contract, by the FPA2007-66665-C02-01/ and FPA2010-16963 projects (Spain), and is supported by the German Federal Ministry for Education and Re-

search BMBF through Grant No. 05H12GUE.

- [1] G. T. Bodwin, E. Braaten and G. P. Lepage, Phys. Rev. D **51**, 1125 (1995) [Erratum-ibid. D **55**, 5853 (1997)].
- [2] N. Brambilla *et al.* [Quarkonium Working Group], arXiv:hep-ph/0412158; N. Brambilla *et al.*, Eur. Phys. J. C **71**, 1534 (2011).
- [3] B. Aubert *et al.* [BABAR Collaboration], Phys. Rev. Lett. **87**, 162002 (2001).
- [4] K. Abe *et al.* [BELLE Collaboration], Phys. Rev. Lett. **88**, 052001 (2002).
- [5] K. Abe *et al.* [Belle Collaboration], Phys. Rev. Lett. **89**, 142001 (2002); K. Abe *et al.* [Belle Collaboration], Phys. Rev. D **70**, 071102 (2004);
- [6] P. Pakhlov *et al.* [Belle Collaboration], Phys. Rev. D **79**, 071101 (2009).
- [7] B. Aubert *et al.* [BABAR Collaboration], Phys. Rev. D **72**, 031101 (2005).
- [8] P. L. Cho and A. K. Leibovich, Phys. Rev. D **54**, 6690 (1996); S. Baek, P. Ko, J. Lee and H. S. Song, J. Korean Phys. Soc. **33**, 97 (1998);
- [9] K. Y. Liu, Z. G. He and K. T. Chao, Phys. Rev. D **69**, 094027 (2004).
- [10] E. Braaten and J. Lee, Phys. Rev. D **67**, 054007 (2003) [Erratum-ibid. D **72**, 099901 (2005)]; K. Y. Liu, Z. G. He and K. T. Chao, Phys. Lett. B **557**, 45 (2003).
- [11] Y. J. Zhang, Y. j. Gao and K. T. Chao, Phys. Rev. Lett. **96**, 092001 (2006); Y. J. Zhang and K. T. Chao, Phys. Rev. Lett. **98**, 092003 (2007); Y. J. Zhang, Y. Q. Ma and K. T. Chao, Phys. Rev. D **78**, 054006 (2008).
- [12] B. Gong and J. X. Wang, Phys. Rev. D **77**, 054028 (2008); B. Gong and J. X. Wang, Phys. Rev. Lett. **100**, 181803 (2008); B. Gong and J. X. Wang, Phys. Rev. D **80**, 054015 (2009).
- [13] G. T. Bodwin, D. Kang, T. Kim, J. Lee and C. Yu, AIP Conf. Proc. **892**, 315 (2007); Z. G. He, Y. Fan and K. T. Chao, Phys. Rev. D **75**, 074011 (2007).
- [14] E. Braaten and Y. Q. Chen, Phys. Rev. Lett. **76**, 730 (1996);
- [15] F. Yuan, C. F. Qiao and K. T. Chao, Phys. Rev. D **56**, 321 (1997);
- [16] S. Fleming, A. K. Leibovich and T. Mehen, Phys. Rev. D **68**, 094011 (2003);
- [17] J. X. Wang, arXiv:hep-ph/0311292;
- [18] V. M. Driesen, J. H. Kuhn and E. Mirkes, Phys. Rev. D **49**, 3197 (1994).
- [19] Y. Q. Ma, Y. J. Zhang and K. T. Chao, Phys. Rev. Lett. **102**, 162002 (2009);

- [20] B. Gong and J. X. Wang, Phys. Rev. Lett. **102**, 162003 (2009).
- [21] Y. J. Zhang, Y. Q. Ma, K. Wang and K. T. Chao, Phys. Rev. D **81**, 034015 (2010).
- [22] Z. G. He, Y. Fan and K. T. Chao, Phys. Rev. D **81**, 054036 (2010).
- [23] Y. Jia, Phys. Rev. D **82**, 034017 (2010).
- [24] R. Li and J. X. Wang, Phys. Rev. D **82**, 054006 (2010).
- [25] Z. G. He and J. X. Wang, Phys. Rev. D **81**, 054030 (2010); Z. G. He and J. X. Wang, Phys. Rev. D **82**, 094033 (2010).
- [26] P. Artoisenet, J. M. Campbell, F. Maltoni and F. Tramontano, Phys. Rev. Lett. **102**, 142001 (2009).
- [27] C. H. Chang, R. Li and J. X. Wang, Phys. Rev. D **80**, 034020 (2009).
- [28] M. Butenschoen and B. A. Kniehl, Phys. Rev. Lett. **104**, 072001 (2010).
- [29] J. M. Campbell, F. Maltoni and F. Tramontano, Phys. Rev. Lett. **98**, 252002 (2007).
- [30] B. Gong and J. X. Wang, Phys. Rev. Lett. **100**, 232001 (2008).
- [31] B. Gong and J. X. Wang, Phys. Rev. D **78**, 074011 (2008).
- [32] E. Braaten and S. Fleming, Phys. Rev. Lett. **74**, 3327 (1995).
- [33] B. Gong, X. Q. Li and J. X. Wang, Phys. Lett. B **673**, 197 (2009).
- [34] Y. Q. Ma, K. Wang and K. T. Chao, Phys. Rev. Lett. **106**, 042002 (2011).
- [35] M. Butenschoen and B. A. Kniehl, Phys. Rev. Lett. **106**, 022003 (2011).
- [36] M. Benayoun, S. I. Eidelman, V. N. Ivanchenko and Z. K. Silagadze, Mod. Phys. Lett. A **14**, 2605 (1999).
- [37] C. H. Chang, C. F. Qiao and J. X. Wang, Phys. Rev. D **56**, 1363 (1997);
- [38] C. H. Chang, C. F. Qiao and J. X. Wang, Phys. Rev. D **57**, 4035 (1998).
- [39] T. Mannel and R. Urech, Z. Phys. C **73**, 541 (1997).
- [40] J. Z. Bai *et al.* [BES Collaboration], Phys. Rev. D **62**, 032002 (2000).
- [41] K. Nakamura *et al.* [Particle Data Group], J. Phys. G **37**, 075021 (2010).
- [42] J. X. Wang, Nucl. Instrum. Meth. A **534**, 241 (2004).
- [43] Y. J. Zhang, B. Q. Li and K. Y. Liu, arXiv:1003.5566 [hep-ph].
- [44] M. Butenschoen and B. A. Kniehl, arXiv:1105.0820 [hep-ph].
- [45] M. Butenschoen and B. A. Kniehl, Phys. Rev. Lett. **108**, 172002 (2012).
- [46] K. -T. Chao, Y. -Q. Ma, H. -S. Shao, K. Wang and Y. -J. Zhang, Phys. Rev. Lett. **108**, 242004 (2012).

[47] B. Gong, L. -P. Wan, J. -X. Wang and H. -F. Zhang, arXiv:1205.6682 [hep-ph].